Polarization transfer in hard x-ray Rayleigh scattering for non-coplanar geometry

Wilko Middents,[1,2,3,*] Alexandre Gumberidze,[1] Thomas Krings,[4] Anton Kononov,[1] Philip Pfäfflein,[1,2,3,†] Norbert Schell,[5] Uwe Spillmann,[1] Sophia Strnat,[6,7,‡] Andrey Surzhykov,[6,7] Marco Vockert,[2,3] Andrey Volotka,[1,2,§] Günter Weber,[1,2] Vladimir A Yerokhin,[8] and Thomas Stöhlker[1,2,3]

[1]*GSI Helmholtzzentrum für Schwerionenforschung GmbH, Planckstraße 1, D-64291 Darmstadt, Germany*
[2]*Helmholtz Institute Jena, Fröbelstieg 3, D-07743 Jena, Germany*
[3]*Institute of Optics and Quantum Electronics, Friedrich Schiller University Jena, Max-Wien-Platz 1, D-07743 Jena, Germany*
[4]*Institut für Kernphysik, Forschungszentrum Jülich, D-52425 Jülich, Germany*
[5]*Institute of Materials Physics, Helmholtz-Zentrum Hereon, Max Planck Strasse 1, D-21502 Geesthacht, Germany*
[6]*Physikalisch-Technische Bundesanstalt, D-38116 Braunschweig, Germany*
[7]*Technische Universität Braunschweig, Institut für Mathematische Physik, D-38106 Braunschweig, Germany*
[8]*Max Planck Institute for Nuclear Physics, Saupfercheckweg 1, D-69117 Heidelberg, Germany*

(Received 10 October 2025; accepted 17 December 2025; published 21 January 2026)

We present an experimental study of the Rayleigh scattering of highly linearly polarized hard x rays. For this study, photons produced by a synchrotron source with an energy of 175 keV are scattered by a thin gold foil target. While the linear polarization in terms of degree of polarization and its orientation of the incident photon beam are well known, the outgoing scattered photons are analyzed by means of Compton polarimetry. For this, a polarimeter detector is positioned at different observation angles with respect to the incident photon beam. For the first time the polarization of elastically scattered photons outside of the polarization plane of the incident radiation is investigated, enabling novel access to a so-far untested component of the polarization transfer. The experimental findings are compared to predictions of two theoretical models. It is found that, when leaving the polarization plane of the incident photon beam, a strong deviation from the form factor approximation is evident, while calculations of the Rayleigh scattering in the *S*-matrix approach agree with the experimental results. Furthermore, this study is a foundation for future experiments dedicated to a polarization-resolved analysis of Delbrück scattering.

DOI: 10.1103/sfnd-hv3k

I. INTRODUCTION

Elastic photon scattering is the fundamental photon-matter interaction process in which the incident and scattered photons carry the same energy $\hbar\omega$. The dominant elastic photon scattering channel for energies up to the MeV range is Rayleigh scattering by bound electrons [1,2]. At higher photon energies, the elastic scattering by the electromagnetic field of the nucleus (Delbrück scattering) [3] and nuclear scattering phenomena [4,5] become important. Extensive reviews of the elastic photon scattering processes can be found, for example, in the work of Kane *et al.* [6], Roy *et al.* [7], or Bradley *et al.* [8]. Here we will focus on the core aspects of Rayleigh scattering only, as this is the dominant interaction process in the investigated energy regime. A deep understanding of the Rayleigh scattering is also essential for detailed studies of the other elastic scattering channels as the observed phenomena result from a superposition of all relevant channels. This is of special interest due to the recent progress in the description of Delbrück scattering [9,10], which for the first time provides all-order calculations of the scattering process, resolving a long-standing discrepancy with experiments. Moreover, it was recently predicted that the interplay of Rayleigh scattering and Delbrück scattering results in distinct polarization characteristics that might provide sensitity to Delbürck scattering even at relatively low energies of below 1 MeV [11]. For a complete understanding of Rayleigh scattering, not only the evaluation of the total and angle-differential scattering cross section is of interest, but also the polarization transfer from the incident to the scattered photon beam needs to be explored. This was the focus of recent theoretical investigations [12–17], which showed the importance of polarization-sensitive measurements for a complete understanding of the Rayleigh scattering. It was also shown that the analysis of Rayleigh scattering can be used for testing the polarization purity of a hard x-ray beam [18,19]. Furthermore, it was

*Contact author: wilko.middents@uni-jena.de
†Present address: European XFEL, Holzkoppel 4, D-22869, Schenefeld, Germany.
‡Present address: Tampere University, Photonics Laboratory, Physics Unit, Tampere, FI-33014, Finland.
§Present address: School of Physics and Engineering, ITMO University, 197101 St. Petersburg, Russia.

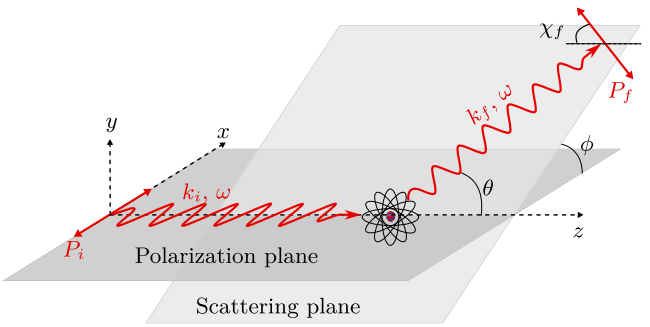

FIG. 1. Geometry of Rayleigh scattering of a linearly polarized photon beam. The incident photons propagate along the z axis. The polarization plane of the incident photon beam is chosen as reference. The wave vectors of the incident and scattered photons k_i and k_f span the scattering plane. The scattered photon direction is defined by the polar and azimuthal scattering angles θ and ϕ. The polarization vector of the scattered photons is defined with respect to the scattering plane with the polarization angle χ_f.

suggested recently to exploit the transfer from circular to linear polarization in Rayleigh scattering for a diagnostics for circular polarization of hard x rays [20]. These Rayleigh-scattering-based diagnostic methods rely on a good understanding of the polarization transfer from incident to scattered photon beam and thus a thorough test of the underlying model is essential.

Until recently, measurements of the Rayleigh scattering of hard x rays, which also include the polarization-dependent behavior, were scarce. Experimentally, this analysis was hampered due to the lack of highly polarized, intense hard x-ray sources and of efficient polarization-sensitive diagnostics tools. Also, aking into account the rather low interaction cross section of Rayleigh scattering, polarization-sensitive tests of hard x-ray Rayleigh scattering were limited to two measurement schemes. Either a (partially) polarized incident photon beam was elastically scattered by a target and the anisotropic emission pattern of the scattered photons was detected or photons of an unpolarized source were elastically scattered and the scattered photons were investigated for their linear polarization by a polarimeter [12].

With the advent of third-generation synchrotron sources, highly brilliant, highly intense hard x-ray sources with photon energies up to several 100 keV became available. Furthermore, the development of segmented semiconductor detectors as dedicated Compton polarimeters [21–24] allowed for efficient linear polarization measurements in the hard x-ray regime. Combining these two technologies, it was possible to perform a first experimental investigation of the polarization transfer from a highly linearly polarized incident photon beam to the to scattered photon beam in Rayleigh scattering [25]. In this pioneering study, both the linear polarization of the incident and scattered photon beam were determined independently. However, only scattering within the polarization plane of the incident photon beam (as defined by the propagation direction and linear polarization orientation of the photon beam, see Fig. 1) was analyzed. For a complete test of Rayleigh scattering, however, the scattering out of the incident polarization plane also needs to be accessed [16,17,19]. In this work, we extend the previous study by investigating the polarization transfer in the Rayleigh scattering of hard x rays for nonzero azimuthal scattering angles (where the azimuthal scattering angle is the angle between the scattering plane and the polarization plane of the incident photon beam, see Fig. 1). For this purpose, we performed an experiment at the beamline P07 of the synchrotron facility PETRA III at DESY [26], scattering a highly linearly polarized synchrotron beam by a gold foil target. Certain results of this beamtime focusing on the angle-differential scattering cross section of Rayleigh scattering [27] and on the polarization transfer in Compton scattering [28] were already published. In this work, we focus on the polarization transfer in the elastic scattering by the gold target. We will briefly discuss the theory of Rayleigh scattering in Sec. II. In Sec. III the experiment and data analysis are discussed and the results will be presented in Sec. IV.

II. HARD X-RAY RAYLEIGH SCATTERING

For an extensive review of the theoretical framework, please see [2,6,7,16,17,19]. Here, we will only introduce the main concepts of Rayleigh scattering necessary for our work by limiting the description to the case of a (partially) linearly polarized incident photon beam. We begin by defining the geometry of the scattering process as presented in Fig. 1.

For an experiment at a synchrotron facility, as presented in this work the incident photon beam is (partially) linearly polarized with a degree of linear polarization $P_{l,i}$ within the plane of the synchrotron ring. Thus, it is convenient to choose the plane of the synchrotron ring and with this the polarization plane of the incident photon beam as a reference plane. The incident photon beam propagates along the z axis in this reference plane. The propagation direction of the scattered photons is characterized by the polar and azimuthal scattering angles θ and ϕ. Here, θ is the angle between the wave vectors k_i and k_f of the incident and scattered photon beams and ϕ is the angle between the polarization plane of the incident photon beam and the scattering plane (see Fig. 1).

The linear polarization of the scattered photon beam can be characterized by the degree of linear polarization $P_{L,f}$ and a polarization angle χ_f. Here, χ_f is conveniently defined with respect to the scattering plane. From the degree of linear polarization and the polarization angle the Stokes parameters P_1 and P_2 can also be determined

$$P_{1,f} = P_{L,f} \times \cos(2\chi_f), \tag{1}$$

$$P_{2,f} = P_{L,f} \times \sin(2\chi_f). \tag{2}$$

In theory, the Rayleigh scattering off closed-shell atoms can be described by the scattering amplitudes $\mathscr{A}_\parallel$ and $\mathscr{A}_\perp$, which correspond to the scattering of photons polarized within and perpendicular to the scattering plane [12]. Several theoretical approximations are known for the evaluation of these amplitudes. The simple form factor approach [29] is based on a modification of the Thomson scattering, i.e., the scattering of photons by a free point-like charge, where the form factor accounts for the charge distribution of the bound electrons. Various methods for the calculation of the form factors were established and can be found in the literature [7,30]. Being based on the Thomson scattering and thus on dipole

emission characteristics, all these approaches have in common that the resulting scattering amplitudes are related via $\mathscr{A}_{\parallel} = \mathscr{A}_{\perp}\cos(\theta)$. This implies no scattering under $\theta = 90^{\circ}$ within the polarization plane of the incident photon beam. In contrast to the form factor approximation, state-of-the-art calculations of the Rayleigh scattering are based on a fully relativistic representation of the scattering process, the *S*-matrix approach. Here, the scattering process is described by an evaluation of the second-order bound-bound transition matrix element. The calculation of this matrix element is discussed extensively in the literature [16–18,31,32]. A separation of the matrix element in its parallel and perpendicular components yields the complex scattering amplitudes $\mathscr{A}_{\parallel}$ and $\mathscr{A}_{\perp}$. Within this fully quantum electrodynamical approach, the minimum in the amplitude $\mathscr{A}_{\parallel}$ is shifted towards a smaller scattering angle. Also, the above-mentioned correlation of the scattering amplitudes is absent, resulting in a finite scattering cross section in this minimum.

By making use of the scattering amplitudes, one can express the differential cross section of Rayleigh scattering of (partially) linearly polarized incident x rays as [27]

$$\left(\frac{d\sigma}{d\Omega}\right)_R = T_{00} + [P_{L,i}\cos(2\phi)]T_{01}, \tag{3}$$

with $T_{00} = \frac{1}{2}(|\mathscr{A}_{\parallel}|^2 + |\mathscr{A}_{\perp}|^2)$ and $T_{01} = \frac{1}{2}(|\mathscr{A}_{\parallel}|^2 - |\mathscr{A}_{\perp}|^2)$. Similarly, the Stokes parameters for linear polarization of the scattered photon beam are given by [13,19,33]

$$P_{1,f} = \frac{T_{01} + P_{L,i}\cos(2\phi)T_{00}}{T_{00} + P_{L,i}\cos(2\phi)T_{01}}, \tag{4}$$

$$P_{2,f} = \frac{P_{L,i}\sin(2\phi)T_{22}}{T_{00} + P_{L,i}\cos(2\phi)T_{01}}, \tag{5}$$

with $T_{22} = \Re(\mathscr{A}_{\parallel}\mathscr{A}_{\perp}^{*})$, where $\Re$ means the real part of the complex amplitude.

Equations (3) to (5) show, that a complete test of Rayleigh scattering of linearly polarized photons includes a determination of the polarization transfer from incident to scattered photons both for scattering within and out of the polarization plane of the incident photon beam. For Rayleigh scattering of a (partially) linearly polarized photon beam under nonzero azimuthal scattering angles, the Stokes parameter $P_{2,f}$ becomes nonzero. This enables not only a test of the absolute values of the scattering amplitudes $\mathscr{A}_{\parallel}$ and $\mathscr{A}_{\perp}$ but also of their phase. A special case is scattering at an inclination of $\phi = 45^{\circ}$ and $\phi = 135^{\circ}$ with respect to the linear polarization of the incident photon beam. Here, both the angle-differential scattering cross section of Rayleigh scattering and the Stokes parameter $P_{1,f}$ become independent from the polarization of the incident photon beam. This enables a "pure" test of the absolute values of the Rayleigh scattering amplitudes (without influences due to polarization impurities).

III. EXPERIMENT AND DATA ANALYSIS

In our work, we extend the previous study by Blumenhagen *et al.* [25] and perform an experiment at the High Energy Materials Science Beamline P07 at the synchrotron facility PETRA III at DESY [26]. A detailed description of the experimental setup can be found in [27], thus here we only briefly describe the main concept. In the experiment the synchrotron beam was scattered by a thin gold ($Z = 79$) foil target with a thickness of $d = 1\,\mu$m. The photon energy of the synchrotron beam was set to $\hbar\omega = 175\,$keV. This photon energy is low enough that Rayleigh scattering is the dominant elastic scattering process and other channels as Delbrück scattering can be neglected [11] and high enough that relativistic effects have a strong influence on the scattering process and need to be included in the calculation of the scattering process. The incident synchrotron beam is highly linearly polarized within the plane of the synchrotron ring. From an evaluation of the linear polarization of the Compton scattered radiation [28], the Stokes parameters of the incident synchrotron beam within the plane of the synchrotron ring could be determined as $P_{1,i} = 0.9896 \pm 0.0063$ and $P_{2,i} = 0.012 \pm 0.018 \approx 0$. $P_{2,i}$ being consistent with zero is a result of choosing the reference plane of the experiment to be identical with the polarization plane of the incident photon beam. The scattered radiation was detected by two detectors, a high purity germanium detector and a two-dimensional (2D) sensitive lithium-diffused silicon strip detector [24].

TABLE I. Different observation angles of the Compton polarimeter used in the experiment at PETRA III [27]. The uncertainties of the polar and azimuthal scattering angles θ and ϕ are 0.1° and 1°, respectively.

θ	63.4°	65.2°	88.2°	71.7°	89.1°
ϕ	0	158°	161°	133°	136°

In this work, we are only interested in the measurement with the 2D sensitive detector. It consists of a Si (Li) crystal with both the front and back side being segmented in a structure of 32 strips each. Each strip has a width of 1 mm and the strips on front and back side are oriented perpendicular to each other, resulting in an active area of 32 mm × 32 mm. As each of these strips is read out individually and thus can act as an individual detector, the strip structure leads to a grid of 1024 pseudopixels resulting in a 2D position-sensitive detector with an energy resolution of 1 keV full width at half maximum (FWHM) at a reference energy of 60 keV. The detector was positioned under various polar scattering angles θ both within the plane of the synchrotron ring ($\phi = 0$) and out of it ($\phi \neq 0$). The observation angles are summarized in Table I. The detector was positioned at a distance of about 50 cm from the gold foil target, resulting in a half opening angle of $\approx 2^{\circ}$.

An example energy spectrum from the experiment obtained with the Compton polarimeter positioned at $\theta = 65.2^{\circ}$, $\phi = 158^{\circ}$ is shown in Fig. 2. For the displayed spectrum, only so-called single-hit events within the detector are evaluated, meaning events where only one strip of the detector on both the front and back sides register an energy deposition. These events are due to the direct photoabsorption of the detected photon within the detector crystal. The spectrum is not corrected for the detection efficiency of the Compton polarimeter. Besides from the Rayleigh peak for elastic scattering at 175 keV (i.e., the photon energy of the incident synchrotron beam), the spectrum also shows the broad Compton peak, that stems from inelastic scattering by the

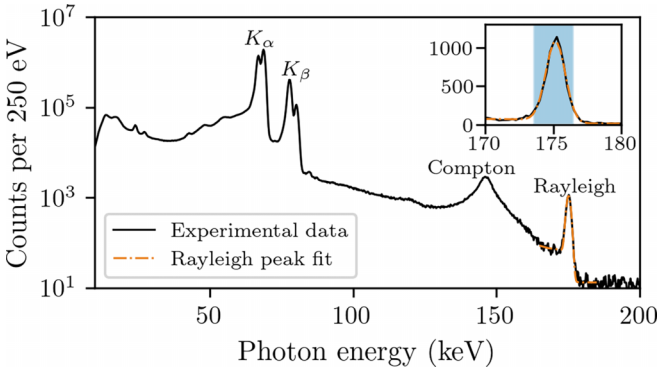

FIG. 2. Energy-resolved spectrum of 175 keV photons scattered by gold, obtained from single-hit events within the Compton polarimeter positioned at $\theta = 65.2°$, $\phi = 158°$. The spectrum is not corrected for the efficiency of the detector. The inset plot shows a zoom to the Rayleigh peak, the shaded area highlights the area of interest for the polarization analysis.

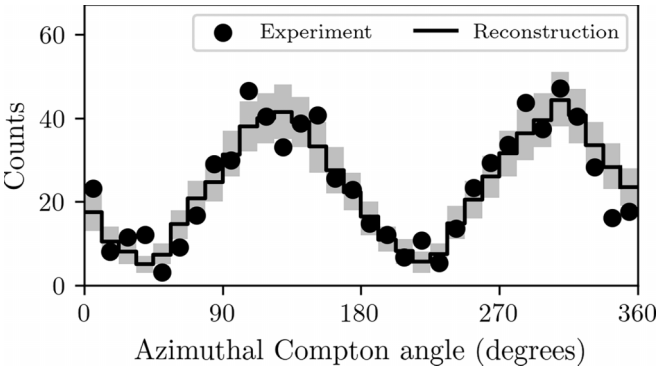

FIG. 3. Azimuthal distribution of Compton scattering within the detector positioned at $\theta = 65.2°$, $\phi = 158°$. The events are limited to x rays being Rayleigh scattered by the gold target. For a better visual representation, the distribution was corrected for geometrical and binning effects. Additionally, a reconstruction of the azimuthal distribution is displayed with a probability interval of 0.68 (shaded area).

gold target and the characteristic fluorescence lines K_α and K_β from the gold target. For better visibility, the inset plot shows a zoom to the Rayleigh peak. Along the experimental spectrum, an adjustment of a model function to the Rayleigh peak using a least-squares minimization is displayed. The model is based on a Gaussian-shaped peak profile, combined with a step-function for the detector response, a term for the high-energy tail of the Compton peak [28] and a constant offset for the background. This adjustment can be used to estimate the influence of the background on the polarization measurements as discussed further below. The blue shaded area around the Rayleigh peak highlights the energy region of interest for the polarization determination of the Rayleigh scattered x rays.

It has been shown that the detector setup based on a double-sided segmented structure can be utilized for efficient Compton polarimetry [21,23,24,34]. It was used for this purpose in a wide variety of experiments in the field of atomic physics in the past two decades, e.g., [25,28,35–40]. An overview of the concept of Compton polarimetry, which was first demonstrated by Metzger and Deutsch [41], was presented by Lei *et al.* [42]. For this purpose, instead of the single-hit events, double-hit events need to be evaluated. This means the registration of an energy deposition at two positions within the detector crystal. To avoid events which originate from charge sharing between two strips, double-hit events from neighboring strips are omitted in our analysis [21]. If the registered energies fit to the energy relation of Compton scattering (see Eq. (2.30) in [42]), these events can most likely be linked to Compton scattering within the detector crystal, where both the energy given to the recoil electron is registered at the position of scattering and the scattered photon is absorbed subsequently at a different position. From the energy information of each strip, the total energy of the incident detected photon and the positions of the recoil electron and of the absorbed scattered photon can be determined. This results in the scattering distribution of Compton scattering within the detector crystal. From the Klein-Nishina formula [43,44] it can be seen that the resulting azimuthal scattering pattern is sensitive to the linear polarization of the analyzed radiation. Scattering perpendicular to the electric field vector is pronounced and scattering in a parallel direction is suppressed. Thus, from the azimuthal scattering distribution of Compton scattering, the degree of linear polarization of the detected x-ray beam can be determined as well as its orientation with respect to the detector axes.

Limiting the events to a particular energy range, only certain spectral features of the impinging radiation can be analyzed. Here, since the radiation being Rayleigh scattered by the gold target is of interest, as highlighted in Fig. 2, only events with a total energy deposition of (175 ± 1.5)keV are accepted. An example of azimuthal distribution of Compton scattering within the detector crystal is displayed in Fig. 3. The distribution stems from x rays that are Rayleigh scattered by the gold target at $\theta = 65.2°$, $\phi = 158°$.

A common approach to determine the linear polarization of the analyzed photon beam is the adjustment of an analytical function based on the Klein-Nishina formula to the azimuthal Compton distribution, resulting in the degree of linear polarization P_L and polarization angle χ [45,46]. This method, however, depends on a correction of the detector-dependent effects (such as pixel structure and energy resolution) to provide reliable results. Additionally, apart from real Compton events within the detector crystal, spurious events from a random coincident detection of two independent photons within the detector that fulfill the conditions for Compton scattering can occur. The analytical reconstruction method cannot correct for these events to a satisfying degree, even if a correction factor according to [45] is included. An alternative approach for the polarization reconstruction is used here based on Monte Carlo simulated reference Compton distributions with defined linear polarization states. The reference distributions are obtained by a simulation using the EGS5 Monte Carlo code for photon and electron transport in matter [47]. This simulation has shown to be able to reproduce all features of the response of the detector crystal in great detail [48]. The used reconstruction algorithm is presented and discussed in detail in [49] and can precisely reproduce the linear

polarization of the investigated photon beam based solely on the Monte Carlo simulated reference distributions, resulting in the Stokes parameters P_1 and P_2 of the analyzed photon beam. Figure 3 also shows the reconstructed azimuthal Compton distribution from this analysis.

In addition to the random coincident double hits, which are corrected for in the analysis, real background events can also hit the detector and contribute to the measured data. These events are strongly reduced by guiding the incident and scattered photon beam in a vacuum, extensive lead shielding at the beam collimator and at the entrance and exit ports of the vacuum chamber and around the detector itself. However, residual background events can occur. These dominantly stem from the high-energy tail of the Compton peak and multiple scattering (e.g., first from the collimator under a very low scattering angle and then from the gold target or target holder under a scattering angle close to the observation angle) and natural radiation (which is quite low, as can be seen in Fig. 2 on the high-energy side of the Rayleigh peak). The registered (real) background events that undergo Compton scattering within the detector crystal will show a certain linear polarization based on the superposition of all events. Thus, the measured Stokes parameters in the energy region of the Rayleigh peak are the sum of the Stokes parameters for the Rayleigh scattered photon beam and the Stokes parameters for the background events weighted by the relative intensities of the Rayleigh scattering and background events.

The intensities of the Rayleigh peak and the offset term are determined as the area under the peak profile and the area under the constant offset term resulting from the fit to the Rayleigh peak profile as discussed above and shown in Fig. 2. It is worth noting that the background on the high-energy side of the Rayleigh peak is due to natural radiation, whereas the intensity of the signal on the low-energy side of the Rayleigh peak is not only due to the background, but is also caused by the response function of the detector. The linear polarization of the background contribution cannot be accessed to correct the measured Stokes parameters for Rayleigh scattering. However, the influence of the background can be estimated as an additional contribution to the uncertainty of the Stokes parameters of the Rayleigh scattered photon beam. The above-mentioned contribution from the high-energy tail of the Compton peak to the background exhibits a similar polarization as the Rayleigh peak [28]. The same is true for the multiple scattering events originating from scattering under a small angle from the collimator and then from the gold target or target holder under a similar angle as the observation angle. The (small) contribution due to natural radiation is unpolarized. Further contributions from scattering from other directions is strongly suppressed due to the extensive lead shielding. Thus, it is reasonable to assume that the resulting linear polarization of the background does not differ strongly from the linear polarization of the Rayleigh scattered photon beam. For a rather conservative estimation, we assume the Stokes parameters of the background to lie in a range of ± 0.5 (limited to being ± 1) around the measured Stokes parameters in the Rayleigh peak. With these assumed values, a maximum deviation from the measured Stokes parameters is estimated based on the determined intensities of the Rayleigh scattered events and the background. This deviation is taken into account as additional uncertainty.

IV. RESULTS

Figure 4 displays the Stokes parameters of the photons being elastically scattered by the gold target. As mentioned already above, both Stokes parameters $P_{1,f}$ and $P_{2,f}$ are defined with respect to the scattering plane, formed by the propagation directions of incident and scattered x rays. Next to the experimental data (black markers with error bars) the expected behavior of the Stokes parameters by two different theoretical models is shown assuming a 175 keV incident photon beam being polarized as determined in [28]. The orange curves show the results of a modified form factor approximation with an angle-independent anomalous scattering factor, the corresponding data is obtained from the Rayleigh scattering data base rtab [30]. The blue curves show the results of a calculation of the Rayleigh scattering with the *S*-matrix approach, as described in [16]. The shaded area around the theory curves represents their uncertainties, based on the uncertainty of the linear polarization of the incident photon beam and the uncertainty of the observation angles ($\Delta\theta = 0.1^\circ$, $\Delta\phi = 1^\circ$). The theory predictions are integrated over the solid angle covered by the detector crystal to account for its finite size. While the measured Stokes parameters are in good agreement with the predictions of the *S*-matrix theory for most observation angles, remarkable deviations from the results of modified form factor approximation can be seen. As mentioned above, the form factor approximation is based on the assumption of scattering from a free point charge, resulting in the dipole emission of the scattered photons. This approximation fails in this study mainly due to the large binding energies of the target electrons in the high-Z target atom, contradicting the assumption of a free target electron. This contradiction is especially pronounced for the chosen large scattering angles, as here contributions from the inner shell electrons dominate the Rayleigh scattering [27]. The mentioned deviations become most pronounced for polar scattering angles around $\theta \approx 90^\circ$, especially for the Stokes parameter $P_{2,f}$. For the form factor approximation, the parallel scattering amplitude is $\mathscr{A}_\parallel = \mathscr{A}_\perp \cos\theta$, thus here $P_{2,f}$ is expected to be 0 at $\theta = 90^\circ$ for any polarization of the incident photon beam. Within the *S*-matrix approach, the mentioned limitations of the form factor approximation are overcome as the scattering process is calculated in the framework of quantum electrodynamics. From this, the simple $\cos(\theta)$ relation between the scattering amplitudes $\mathscr{A}_\parallel$ and $\mathscr{A}_\perp$ does not hold anymore. Additionally, the minimum of $\mathscr{A}_\parallel$ (both the real and imaginary parts) is shifted to lower polar scattering angles, thus also shifting both the minimum of $P_{1,f}$ and the zero-crossing of the Stokes parameter $P_{2,f}$.

Table II shows the values for the measured Stokes parameters of the photons being elastically scattered by the gold target. The displayed uncertainty of the experimental values is separated into a part from the analysis of the Compton scattering distribution (labeled with "r"), whereas the additional influence of the unknown background polarization is indicated with "b" and separated into a positive and negative influence.

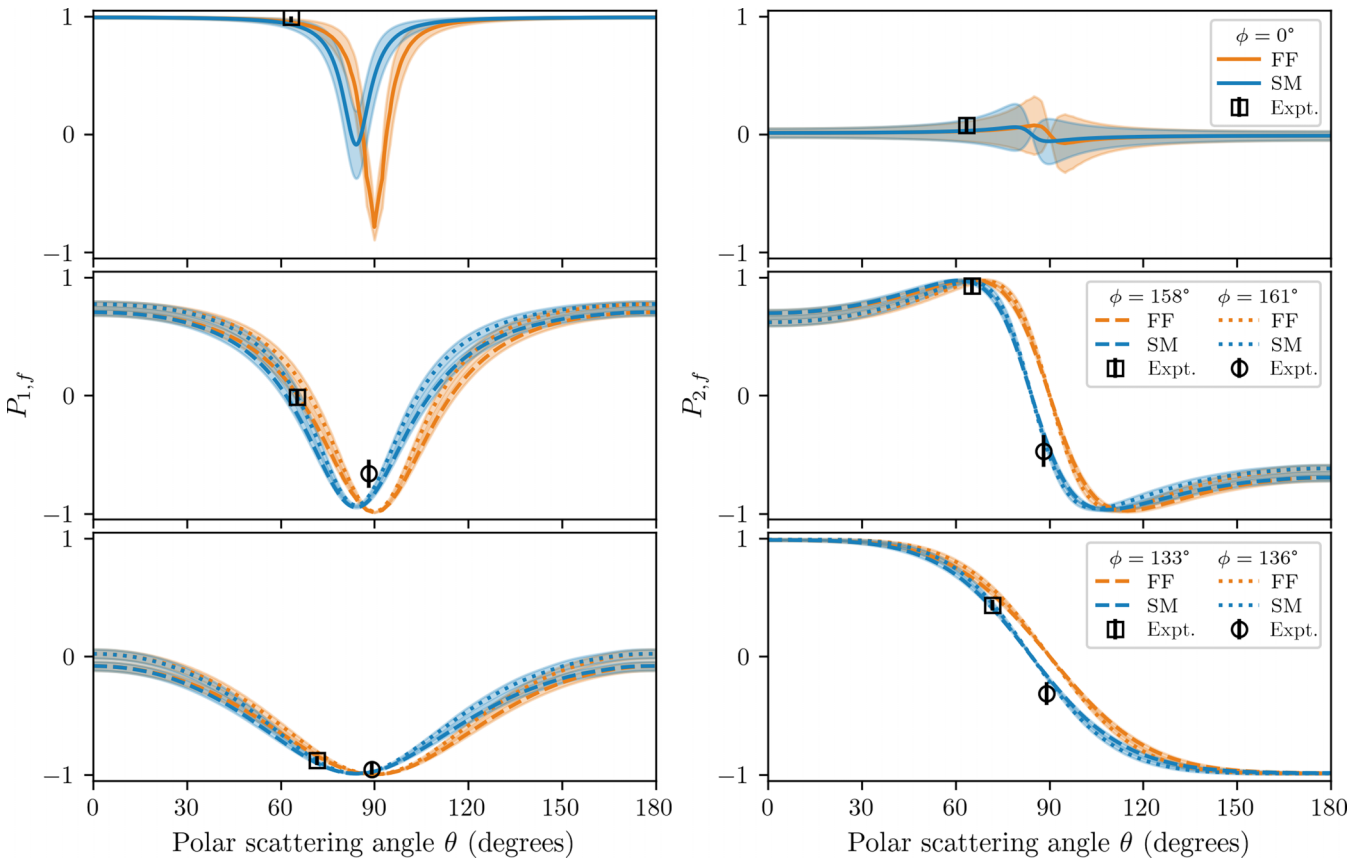

FIG. 4. Stokes parameters $P_{1,f}$ (left) and $P_{2,f}$ (right) of the Rayleigh-scattered photon beam for both experimental data (black errorbars) and theoretical models based on a modified form factor with angle-independent anomalous scattering factor [30] (orange) and on the S matrix [16] (blue), the shaded area shows the corresponding uncertainties. The theory curves are shown for an extended detector. Each row represents results for similar azimuthal scattering angles, top: $\phi = 0$, middle: $\phi \approx 160°$, bottom: $\phi \approx 135°$.

Additionally, Table II presents the predictions for the Stokes parameters calculated within both theoretical models, i.e., the form factor approximation and the S-matrix approach. Again, the theory values are shown integrated over the solid angle covered by the detector crystal. For a better visualization of the comparison between the measured Stokes parameters and the theory values, predicted in the S-matrix approach, their difference is shown in Fig. 5.

As already discussed above, the experimentally obtained Stokes parameters agree well within their uncertainties with the theory values calculated in the S-matrix approach for most observation angles. The stronger deviations for $P_{1,f}$ at the

TABLE II. Stokes parameters of the Rayleigh-scattered photon beam. The experimental uncertainty is seperated in two parts, one due to the reconstruction (r) and the second due to the unknown background (b). The theory values from the form factor approximation [30] and from the S-matrix model [16] are calculated for the extended detector and for $P_{1,i} = 0.9896 \pm 0.0063$, $P_{2,i} = 0.012 \pm 0.018$ [28].

(θ, ϕ)		Experiment	Form factor	S matrix
(63.4°, 0)	$P_{1,f}$	$0.994(46)_r(^{+06}_{-00})_b$	0.941(35)	0.930(41)
	$P_{2,f}$	$0.079(67)_r(^{+14}_{-14})_b$	0.028(90)	0.030(97)
(65.2°, 158°)	$P_{1,f}$	$-0.015(59)_r(^{+15}_{-15})_b$	−0.08(16)	−0.15(17)
	$P_{2,f}$	$0.925(50)_r(^{+15}_{-02})_b$	0.973(74)	−0.957(92)
(88.2°, 161°)	$P_{1,f}$	$-0.66(11)_r(^{+03}_{-05})_b$	−0.9896(37)	−0.853(44)
	$P_{2,f}$	$-0.47(13)_r(^{+03}_{-05})_b$	0.00393(77)	−0.367(55)
(71.7°, 133°)	$P_{1,f}$	$-0.881(37)_r(^{+02}_{-07})_b$	−0.856(24)	−0.904(20)
	$P_{2,f}$	$0.435(46)_r(^{+07}_{-07})_b$	0.511(84)	0.410(76)
(89.1°, 136°)	$P_{1,f}$	$-0.954(65)_r(^{+02}_{-17})_b$	−0.99860(10)	−0.9734(37)
	$P_{2,f}$	$-0.315(96)_r(^{+17}_{-17})_b$	0.001471(52)	−0.179(15)

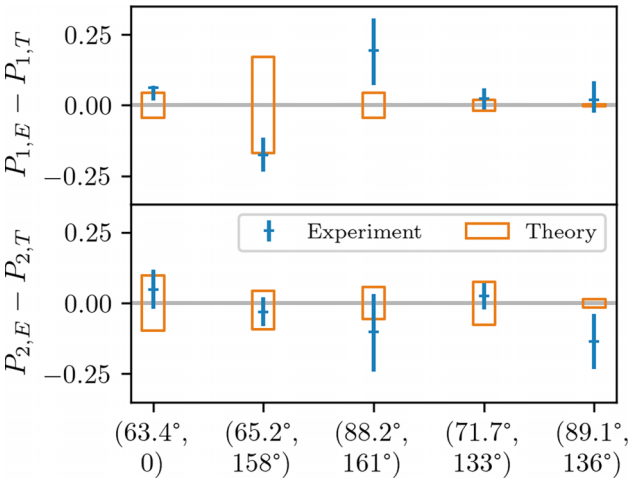

FIG. 5. Difference of the measured Stokes parameters of the Rayleigh scattered photons and the theoretical predictions from the *S*-matrix approach. The length of the blue error bars is given by the root sum squared of the individual experimental uncertainties, the theoretical uncertainty is indicated by the orange boxes.

observation angles ($\theta = 88.2°, \phi = 158°$) and for $P_{2,f}$ at ($\theta = 89.1°, \phi = 136°$) can be explained by statistical effects. However, it is also worth noting that for these observation angles the Rayleigh scattering cross section is lowest compared to the other angles [27]. Thus, effects from the unknown background will probably be most pronounced and might influence the detected polarization stronger than estimated.

V. CONCLUSION AND OUTLOOK

In summary, the Rayleigh scattering of strongly linearly polarized x rays off a thin gold foil was measured at the PETRA III synchrotron facility in Hamburg, Germany. In this experiment, special attention was paid to the transfer of polarization from incident to scattered photons. The performed measurements provided the very first test of hard x-ray Rayleigh scattering, where the polarization of the incident highly linearly polarized hard x rays was controlled and the linear polarization of the scattered photons was analyzed out of the incident photon polarization plane, i.e., for nonzero azimuthal scattering angles ϕ. The novel experimental setup enabled access to a test of both Stokes parameters for linear polarization $P_{1,f}$ and $P_{2,f}$ of the scattered photons. In a comparison of the experimental findings with theoretical predictions, strong deviations between a form factor approximation and the experimental results are evident, in particular for scattering out of the polarization plane of the incident photon and especially for the Stokes parameter $P_{2,f}$ at polar scattering angles $\theta \approx 90°$. State-of-the-art theoretical calculations of Rayleigh scattering based on the *S*-matrix approach, however, agree well with the experimental findings.

This study also serves as a foundation for future experiments focused on the Delbrück channel of elastic scattering, for which all-order (nonperturbative) calculations were recently accomplished [9,10]. Additionally, it was shown that the Delbrück contribution to elastic scattering will indeed also influence the polarization characteristics of the scattered photons, even at photon energies below the pair production limit [11]. For experimental studies of the polarization effects in Delbrück scattering a thorough understanding of the competing elastic scattering processes, i.e., dominantly Rayleigh scattering, as provided by this study, is of utmost importance.

ACKNOWLEDGMENTS

The authors acknowledge financial support from the German Federal Ministry of Education and Research (BMBF) under Grant No. 05P15SJFAA. W.M. acknowledges funding by ErUM FSP T05: "Aufbau von APPA bei FAIR" (BMBF. No. 05P19SJFAA). Support from the SPARC collaboration is acknowledged. Parts of this research were carried out at the light source PETRA III at DESY, a member of the Helmholtz Association (HGF). Support from the GSI Target Laboratory and the GSI Department of Experiment Electronics is acknowledged.

DATA AVAILABILITY

The data that support the findings of this article are not publicly available upon publication because it is not technically feasible and/or the cost of preparing, depositing, and hosting the data would be prohibitive within the terms of this research project. The data are available from the authors upon reasonable request.

[1] W. Franz, Rayleighsche Streuung Harter Strahlung an Schweren Atomen, Z. Phys. **98**, 314 (1935).
[2] S. C. Roy, R. H. Pratt, and L. Kissel, Rayleigh scattering by energetic photons: Development of theory and current status, Radiat. Phys. Chem. **41**, 725 (1993).
[3] L. Meitner and H. Kösters, Über die streuung Kurzwelliger γ-Strahlen, Z. Phys. **84**, 137 (1933).
[4] E. Fuller and E. Hayward, The nuclear photoeffect in Holmium and erbium, Nucl. Phys. **30**, 613 (1962).
[5] Z. Berant, R. Moreh, and S. Kahane, Nuclear Thomson scattering of 5.5–7.2 MeV photons, Phys. Lett. B **69**, 281 (1977).
[6] P. P. Kane, L. Kissel, R. H. Pratt, and S. C. Roy, Elastic scattering of γ-rays and x-rays by atoms, Phys. Rep. **140**, 75 (1986).
[7] S. Roy, L. Kissel, and R. Pratt, Elastic scattering of photons, radiation, Physics and Chemistry **56**, 3 (1999).
[8] D. A. Bradley, O. D. Gonçalves, and P. P. Kane, Measurements of photon-atom elastic scattering cross-sections in the photon energy range 1 keV to 4 MeV, Radiat. Phys. Chem. **56**, 12, 125–150, (1999).
[9] J. Sommerfeldt, V. A. Yerokhin, R. A. Müller, V. A. Zaytsev, A. V. Volotka, and A. Surzhykov, Calculations of Delbrück scattering to all orders in αZ, Phys. Rev. A **105**, 022804 (2022).

[10] J. Sommerfeldt, V. A. Yerokhin, T. Stöhlker, and A. Surzhykov, All-order Coulomb corrections to Delbrück scattering above the pair-production threshold, Phys. Rev. Lett. **131**, 061601 (2023).

[11] J. Sommerfeldt, S. Strnat, V. A. Yerokhin, W. Middents, T. Stöhlker, and A. Surzhykov, Low-energy tests of Delbrück scattering, Phys. Rev. A **108**, 042819 (2023).

[12] S. C. Roy, B. Sarkar, L. D. Kissel, and R. H. Pratt, Polarization effects in elastic photon-atom scattering, Phys. Rev. A **34**, 1178 (1986).

[13] N. L. Manakov, A. V. Meremianin, A. Maquet, and J. P. J. Carney, Photon-polarization effects and their angular dependence in relativistic two-photon bound-bound transitions, J. Phys. B: At. Mol. Opt. Phys. **33**, 4425 (2000).

[14] N. L. Manakov, A. V. Meremianin, J. P. J. Carney, and R. H. Pratt, Circular dichroism effects in atomic x-ray scattering, Phys. Rev. A **61**, 032711 (2000).

[15] A. Surzhykov, V. A. Yerokhin, T. Jahrsetz, P. Amaro, T. Stöhlker, and S. Fritzsche, Polarization correlations in the elastic Rayleigh scattering of photons by hydrogen-like ions, Phys. Rev. A **88**, 062515 (2013).

[16] A. Surzhykov, V. A. Yerokhin, T. Stöhlker, and S. Fritzsche, Rayleigh x-ray scattering from many-electron atoms and ions, J. Phys. B: At. Mol. Opt. Phys. **48**, 144015 (2015).

[17] A. V. Volotka, A. Surzhykov, and S. Fritzsche, Rayleigh scattering of linearly polarized light: Scenario of the complete experiment, Phys. Rev. A **102**, 042814 (2020).

[18] A. Surzhykov, V. A. Yerokhin, S. Fritzsche, and A. V. Volotka, Diagnostics of polarization purity of x rays by means of Rayleigh scattering, Phys. Rev. A **98**, 053403 (2018).

[19] S. Strnat, V. A. Yerokhin, A. V. Volotka, G. Weber, S. Fritzsche, R. A. Müller, and A. Surzhykov, Polarization studies on Rayleigh scattering of hard x rays by closed-Shell atoms, Phys. Rev. A **103**, 012801 (2021).

[20] S. Strnat, J. Sommerfeldt, V. Yerokhin, W. Middents, T. Stöhlker, and A. Surzhykov, Circular polarimetry of hard x-rays with Rayleigh scattering, Atoms, **10**, 140, (2022).

[21] U. Spillmann, H. Bräuning, S. Hess, H. Beyer, T. Stöhlker, J.-C. Dousse, D. Protic, and T. Krings, Performance of a ge-microstrip imaging detector and polarimeter, Rev. Sci. Instrum. **79**, 083101 (2008).

[22] A. Khaplanov, S. Tashenov, B. Cederwall, and G. Jaworski, A γ-ray polarimeter based on a single segmented planar hpge detector, Nucl. Instrum. Methods Phys. Res. Sect. A **593**, 459 (2008).

[23] G. Weber, H. Bräuning, S. Hess, R. Märtin, U. Spillmann, and T. Stöhlker, Performance of a position sensitive Si(Li) x-ray detector dedicated to compton polarimetry of stored and trapped highly-charged ions, J. Instrum. **5**, C07010 (2010).

[24] M. Vockert, G. Weber, U. Spillmann, T. Krings, M. Herdrich, and T. Stöhlker, Commissioning of a Si(Li) compton polarimeter with improved energy resolution, Nucl. Instrum. Methods Phys. Res. Sect. B **408**, 313 (2017).

[25] K.-H. Blumenhagen, S. Fritzsche, T. Gassner, A. Gumberidze, R. Märtin, N. Schell, D. Seipt, U. Spillmann, A. Surzhykov, S. Trotsenko, G. Weber, V. A. Yerokhin, and T. Stöhlker, Polarization transfer in Rayleigh scattering of hard x-rays, New J. Phys. **18**, 103034 (2016).

[26] N. Schell, A. King, F. Beckmann, T. Fischer, M. Müller, and A. Schreyer, The high energy materials science beamline (HEMS) at PETRA III, in *Mechanical Stress Evaluation by Neutrons and Synchrotron Radiation VI, 772 of Materials Science Forum* (Trans Tech, Wollerau, Switzerland, 2014), Vol. 2, pp. 57–61.

[27] W. Middents, G. Weber, A. Gumberidze, C. Hahn, T. Krings, N. Kurz, P. Pfäfflein, N. Schell, U. Spillmann, S. Strnat, M. Vockert, A. Volotka, A. Surzhykov, and T. Stöhlker, Angle-differential cross sections for Rayleigh scattering of highly linearly polarized hard x rays on Au atoms, Phys. Rev. A **107**, 012805 (2023).

[28] W. Middents, A. Gumberidze, T. Krings, T. Over-Winter, P. Pfäfflein, N. Schell, U. Spillmann, M. Vockert, G. Weber, and T. Stöhlker, Linear polarization properties of energetic x-rays being compton-scattered off atomic targets, New J. Phys. **27**, 073204 (2025).

[29] J. H. Hubbell, W. J. Veigele, E. A. Briggs, R. T. Brown, D. T. Cromer, and R. J. Howerton, Atomic form factors, incoherent scattering functions, and photon scattering cross sections, J. Phys. Chem. Ref. Data **4**, 471 (1975).

[30] L. Kissel, RTAB: The Rayleigh scattering database, Radiat. Phys. Chem. **59**, 185 (2000).

[31] R. Pratt, Recent theoretical developments in photon-atom scattering, Radiat. Phys. Chem. **74**, 411 (2005).

[32] L. Safari, P. Amaro, S. Fritzsche, J. P. Santos, and F. Fratini, Relativistic total cross section and angular distribution for Rayleigh scattering by atomic hydrogen, Phys. Rev. A **85**, 043406 (2012).

[33] W. Middents, G. Weber, U. Spillmann, T. Krings, M. Vockert, A. Volotka, A. Surzhykov, and T. Stöhlker, Possible polarization measurements in elastic scattering at the gamma factory utilizing a 2D sensitive strip detector as dedicated compton polarimeter, Ann. Phys. **534**, 2100285 (2022).

[34] G. Weber, H. Bräuning, S. Fritzsche, A. Gumberidze, R. Märtin, R. Reuschl, M. Schwemlein, U. Spillmann, A. Surzhykov, D. F. A. Winters, and T. Stöhlker, Compton polarimeters for the study of hard x-rays arising from energetic collisions of electrons and ions with matter, AIP Conf. Proc. **1438**, 73 (2012).

[35] S. Tashenov, T. Stöhlker, D. Banaś, K. Beckert, P. Beller, H. F. Beyer, F. Bosch, S. Fritzsche, A. Gumberidze, S. Hagmann, C. Kozhuharov, T. Krings, D. Liesen, F. Nolden, D. Protic, D. Sierpowski, U. Spillmann, M. Steck, and A. Surzhykov, First measurement of the linear polarization of radiative electron capture transitions, Phys. Rev. Lett. **97**, 223202 (2006).

[36] S. Hess, H. Bräuning, U. Spillmann, C. Brandau, S. Geyer, S. Hagmann, M. Hegewald, C. Kozhuharov, T. Krings, A. Kumar, R. Märtin, D. Protic, B. O'Rourke, R. Reuschl, M. Trassinelli, S. Trotsenko, G. Weber, D. F. A. Winters, and T. H. Stóhlker, Polarization studies of radiative electron capture into highly charged uranium ions, J. Phys.: Conf. Ser. **163**, 012072 (2009).

[37] M. Vockert, G. Weber, H. Bräuning, A. Surzhykov, C. Brandau, S. Fritzsche, S. Geyer, S. Hagmann, S. Hess, C. Kozhuharov, R. Märtin, N. Petridis, R. Hess, S. Trotsenko, Y. A. Litvinov, J. Glorius, A. Gumberidze, M. Steck, S. Litvinov, T. Gaßner, *et al.*, Radiative electron capture as a tunable source of highly linearly polarized x rays, Phys. Rev. A **99**, 052702 (2019).

[38] G. Weber, H. Bräuning, A. Surzhykov, C. Brandau, S. Fritzsche, S. Geyer, S. Hagmann, S. Hess, C. Kozhuharov, R. Märtin, N. Petridis, R. Reuschl, U. Spillmann, S. Trotsenko, D. F. A. Winters, and T. Stöhlker, Direct determination of the magnetic quadrupole contribution to the Lyman-α_1 transition in a hydrogen-like ion, Phys. Rev. Lett. **105**, 243002 (2010).

[39] S. Tashenov, T. Bäck, R. Barday, B. Cederwall, J. Enders, A. Khaplanov, Y. Poltoratska, K.-U. Schässburger, and A. Surzhykov, Measurement of the correlation between electron spin and photon linear polarization in atomic-field Bremsstrahlung, Phys. Rev. Lett. **107**, 173201 (2011).

[40] R. Märtin, G. Weber, R. Barday, Y. Fritzsche, U. Spillmann, W. Chen, R. D. DuBois, J. Enders, M. Hegewald, S. Hess, A. Surzhykov, D. B. Thorn, S. Trotsenko, M. Wagner, D. F. A. Winters, V. A. Yerokhin, and T. Stöhlker, Polarization transfer of Bremsstrahlung arising from spin-polarized electrons, Phys. Rev. Lett. **108**, 264801 (2012).

[41] F. Metzger and M. Deutsch, A study of the polarization-direction correlation of successive gamma-ray quanta, Phys. Rev. **78**, 551 (1950).

[42] F. Lei, A. J. Dean, and G. L. Hills, Compton polarimetry in gamma-ray astronomy, Space Sci. Rev. **82**, 309 (1997).

[43] O. Klein and T. Nishina, Über die streuung von strahlung durch freie elektronen nach der neuen relativistischen quantendynamik von dirac, Zeitschrift für Physik **52**, 853 (1929).

[44] Y. Yazaki, How the Klein-Nishina formula was derived: Based on the Sangokan Nishina source materials, Proc. Jpn. Acad. Ser. B **93**, 399 (2017).

[45] G. Weber, H. Bräuning, A. Surzhykov, C. Brandau, S. Fritzsche, S. Geyer, R. E. Grisenti, S. Hagmann, C. Hahn, R. Hess, S. Hess, C. Kozhuharov, M. Kühnel, R. Märtin, N. Petridis, U. Spillmann, S. Trotsenko, D. F. A. Winters, and T. Stöhlker, Combined linear polarization and angular distribution measurements of x-rays for precise determination of multipole-mixing in characteristic transitions of high-z systems, J. Phys. B: At. Mol. Opt. Phys. **48**, 144031 (2015).

[46] M. Vockert, G. Weber, U. Spillmann, T. Krings, and T. Stöhlker, Polarization reconstruction algorithm for a compton polarimeter, J. Phys.: Conf. Ser. **1024**, 012041 (2018).

[47] H. Hirayama, Y. Namito, A. F. Bielajew, S. J. Wilderman, M. U., W. R. Nelson, A. Arbor, and W. R. Nelson, The EGS5 Code system, (2005).

[48] G. Weber, H. Bräuning, R. Märtin, U. Spillmann, and T. Stöhlker, Monte Carlo simulations for the characterization of position-sensitive x-ray detectors dedicated to Compton polarimetry, Phys. Scr. **2011**, 014034 (2011).

[49] T. Over-Winter, W. Middents, G. Weber, and T. Stöhlker, Polarization reconstruction based on Monte Carlo simulations for a Compton polarimeter, Atoms **13**, 65 (2025).